Trifluoperazine Binding to Porcine Brain Calmodulin and Skeletal Muscle Troponin C†

Larry Massom, Huey Lee, and Harry W. Jarrett*,‡

Department of Biology, Purdue University School of Science, Indiana University–Purdue University at Indianapolis, Indianapolis, Indiana 46206

Received April 26, 1989; Revised Manuscript Received September 1, 1989

ABSTRACT: Binding of trifluoperazine (TFP), a phenothiazine tranquilizer, to porcine brain calmodulin (CaM) and rabbit skeletal muscle troponin C (Tn C) was measured by an automated high-performance liquid chromatography binding assay using a molecular sieving column; 10 μg of either protein per injection is sufficient for determining TFP binding, and results are comparable to those obtained by equilibrium dialysis. Very little binding was observed to either protein in the absence of Ca^{2+} while in the presence of Ca^{2+} both proteins bind 4 equiv of TFP. Other characteristics of TFP binding however are different for each protein. For CaM, half-maximal binding occurs at 5.8 μM TFP, the Hill coefficient is 0.82, and the fit of the data to the Scatchard equation is consistent with four independent TFP-binding sites. Binding of one melittin displaces two TFP from CaM. Thus, there are two recognizable classes of TFP-binding sites: those that are displaced by melittin and those that are not. TFP causes an increase in the Ca^{2+} affinity of CaM, and three Ca^{2+} must be bound to CaM for TFP binding to occur. The studies also yielded a measure of the intrinsic affinity of three of CaM's Ca^{2+}-binding sites that is in agreement with previous reports. For troponin C, half-maximal binding occurs at 16 μM TFP, the Hill coefficient is 1.7, and the data best fit the Adair equation for four binding sites. The measured constants K_1, K_2, K_3, and K_4 were 2.5×10^4, 6.6×10^3, 5.8×10^5, and 2.0×10^5 M^{-1}, respectively, in 1 mM Ca^{2+} and were similar when Mg^{2+} was additionally included. TFP also increases troponin C's Ca^{2+} affinity, and it is the low-affinity, Ca^{2+}-specific binding sites that are affected. These studies yielded a measure of the intrinsic affinity of these Ca^{2+}-binding sites that is in agreement with previous measurements.

Changes in intracellular Ca^{2+} concentration frequently cause profound effects upon a cell's metabolism. The role of Ca^{2+} in the regulation of muscle contraction, nerve transmission, secretion, and other basic biological processes has long been appreciated. These effects of Ca^{2+} have often been found to be mediated by a class of homologous Ca^{2+}-binding proteins that includes troponin C and calmodulin. CaM[1] is a Ca^{2+}-dependent activator of numerous enzymes while Tn C is a structurally similar protein adapted to the more specialized role of regulating cardiac and skeletal muscle contraction.

TFP, a phenothiazine tranquilizer, is a CaM antagonist effective at micromolar concentrations (Weiss & Levin, 1978). Later, it was discovered that TFP also binds to Tn C (Levin & Weiss, 1978). Other phenothiazines (e.g., chlorpromazine and fluphenazine) (Levin & Weiss, 1978; Silver et al., 1986), a series of naphthylsulfonamide derivatives (Hidaka et al., 1980), and the dye calmidazolium (Silver et al., 1986) are also bound by and effect the biological activity of both Tn C and CaM. TFP and many of these other compounds increase the Ca^{2+} sensitivity of myofilament contraction, and the effect on contractility correlates well with Tn C binding across a series of these compounds (Herzig et al., 1987).

Levin and Weiss (1978) and Marshak et al. (1985) have both measured phenothiazine binding to CaM and arrived at quite different conclusions as to the number of binding sites and the Ca^{2+} dependency of binding. This difference as well as the uncertainty in the number and affinity of drug-binding sites on Tn C led us to reinvestigate drug binding to both proteins.

The number and affinity of these sites are becoming increasingly important as the structure–function relationships involved in drug binding are investigated for both proteins. A drug-binding site on Tn C has been localized to a sequence region (residues 95–102) (Bariépy & Hodges, 1983). The drug-binding regions of CaM have been affinity labeled and the reaction sites sequenced (Newton et al., 1983; Newton & Klee, 1984; Jarrett, 1984; Faust et al., 1987). The latter study showed that Lys^{148}, Lys^{75}, and Lys^{21} all reacted with the affinity label and described a "hydrophobic cup" present in both the amine- and carboxy-terminus halves of CaM which may binding TFP. Studies of drug binding to peptide fragments of CaM agree there is at least one drug-binding site in each half of CaM's sequence (Newton et al., 1984). Several different models have predicted the location of two, high-affinity drug-binding sites located in highly conserved, homologous regions at either end of each protein (Faust et al., 1987; Dalgarno et al., 1984; Klevit et al., 1981; Reid, 1983; Strynadka & James, 1988). The number and affinities of the sites expected for each protein are necessary to evaluate the progress made toward developing a comprehensive model of drug binding for either of these proteins.

Other than the phenothiazine antagonists, CaM also binds several antagonist peptides with high affinity. One such antagonist is melittin, a peptide derived from bee venom (Maulet & Cox, 1983). Here we examine the competition between melittin and TFP for binding to CaM.

† Supported by grants from the National Science Foundation (DMB-8702013) and the National Institutes of Health (GM43609).

‡ Current address: Department of Biochemistry, University of Tennessee, Memphis, TN 38163.

[1] Abbreviations: CaM, porcine brain calmodulin; Tn C, rabbit skeletal muscle troponin C; TFP, trifluoperazine dihydrochloride; EDTA, ethylenediamine-*N*,*N*,*N*′,*N*′-tetraacetic acid; EGTA, ethylene glycol bis(2-aminoethyl ether)-*N*,*N*,*N*′,*N*′-tetraacetic acid; MES, 2-(*N*-morpholino)ethanesulfonic acid; SDS–PAGE, sodium dodecyl sulfate–polyacrylamide gel electrophoresis.

0006-2960/90/0429-671$02.50/0

Hummel and Dreyer (1962) developed a simple, gel filtration binding assay using low-pressure chromatography. A modification of this method has been used to study chlorpromazine binding to CaM (Marshak et al., 1985). Recently, we have adapted this technique to high-pressure liquid chromatography. The new method allows the automated determination of drug binding at different TFP concentrations with as little as 10 μg of protein per injection. Here, this method is described and used to measure TFP binding to CaM and Tn C.

Experimental Procedures

Materials. All chemicals were the highest grade available from Sigma Chemical Co. Imidazole was recrystallized from benzene and then acetone and dried at 50 °C. $CaCl_2$ solutions were prepared by dissolving the carbonate in 2 equiv of HCl. TFP is a mildly light-sensitive compound, and in all of the experiments described, TFP solutions were freshly prepared from the solid just prior to use and filtered through a 0.45-μm filter, the concentration was determined by absorption, and the solution was stored either in brown glass bottles or in containers covered with aluminum foil.

Troponin C from rabbit skeletal muscle was the generous gift of Dr. James Potter (University of Miami). The lyophilized powder was dissolved in 50 mM NH_4HCO_3–1 mM EDTA and dialyzed exhaustively against this buffer. The protein was then dialyzed exhaustively in 10 mM NH_4HCO_3–1 mM 2-mercaptoethanol containing 2 g/L Chelex resin (Sigma Chemical Co., St. Louis, MO). The dialyzed protein was lyophilized in 2-mg aliquots. Immediately prior to use, the protein was redissolved to a concentration of 120 μM in 50 mM imidazole–150 mM KCl, pH 7 (buffer A). This working solution was further diluted to 60 μM with buffers containing Ca^{2+}, Mg^{2+}, or EGTA as appropriate.

Calmodulin was purified from porcine brain by high-pressure affinity chromatography as previously described (Rhoades et al., 1988). Both proteins were of greater than 95% purity as assessed by sodium dodecyl sulfate–polyacrylamide gel electrophoresis (Laemmli, 1970). Protein concentration was by amino acid analysis as previously described (Jarrett et al., 1986).

Equilibrium Dialysis. This and all other binding experiments were at room temperature (20 °C). Tn C was diluted to 12.4 μM, and 0.7-ml aliquots were dialyzed (Spectrapore, 6000 molecular weight cutoff) for 16 h versus buffer A containing additionally 1 mM $CaCl_2$, 3 mM $MgCl_2$, and the TFP concentrations shown in Table I. For comparison, the same buffers and protein solutions were used for the HPLC experiment also described in Table I. After dialysis, the concentration of TFP in both the inside and outside solutions were assayed spectrophotometrically at two different wavelengths (255 and 310 nm) with similar results. For these calculations, we assumed that for TFP E^{M}_{255} = 29 170 M^{-1} cm^{-1} (Jarrett, 1984) and E^{M}_{310} = 3652 M^{-1} cm^{-1} (see Results). The data obtained at 310 nm are used here since this wavelength should suffer less from protein absorption.

High-Performance Liquid Chromatography. The chromatograph was a Gilson Model 9000 binary gradient chromatograph outfitted with a Jasco variable-wavelength UV detector (310 nm, unless otherwise specified), a Gilson 231/401 autosampler, and a 50-μL injector loop. The autosampler was calibrated by repeatedly injecting 10 μL of 2-mercaptoethanol through the column and quantifying the amount recovered by absorption at 220 nm. The sampler delivered 10.09 ± 0.02 μL (n = 6). Data collection and programming of the chromatograph were with a Tandy 3000HD computer and the Gilson 714 software. Buffer A was made to contain the appropriate amounts of Ca^{2+} and Mg^{2+} for each experiment, and buffer B was identical with buffer A except that it contained additionally TFP. The concentration of TFP in buffer B was determined spectrophotometrically at 255 nm. The Bio-Sil TSK-125 column was 7.8 × 300 mm and obtained from Bio-Rad Laboratories (Richmond, CA). All other columns were 4.6 × 100 mm cartridge columns obtained from Alltech/Applied Science (Deerfield, IL). The Rogel P column was 70-Å pore, 5-μm support; the Synchropak and Macrosphere GPC-60 were both 60-Å pore, 7-μm support. All together, four separate Macrosphere GPC-60 columns were used in the course of these studies and were virtually identical with one another in their chromatographic behavior, indicating good reproducibility in these columns.

Automated HPLC Binding Assay. The HPLC column was first equilibrated in buffer A prior to beginning the method. The solvent gradient program is given in Table I of the supplementary material. This program was arrived at empirically and allows the column to be equilibrated at each TFP concentration (i.e., percent buffer B) before injections are made and results in a stable base line for the peaks that must be integrated. The solvent program ends with the reequilibration of the column in buffer A in preparation for the next run. The autoinjector was programmed to deliver 10-μL injections on demand in triplicates spaced 4 min apart. Thus, each injection event represents three injections. The sample for the autoinjector was 300 μL of 60 μM Tn C or CaM in buffer A containing Ca^{2+}, Mg^{2+}, or EGTA as appropriate. Initially, six injections are made at 0% buffer B because infrequently the first sample injected on the column gave a nonreproducible area that was excluded from the data set.

Ca^{2+} Contamination of Buffers. Buffer A containing 10 mM EGTA or 4.1 mM $MgCl_2$–10 mM EGTA was pumped through the column, and the total Ca^{2+} concentration in the effluent was determined by atomic absorption. Either buffer contained ~3 μM Ca^{2+} as determined by atomic absorption, which was used as the buffer Ca^{2+} contamination in our calculations.

Mathematical Apparatus. The equilibrium concentrations of Mg^{2+}, Ca^{2+}, and EGTA were calculated with the program of Perrin and Sayce (1967) and the binding constants listed by Potter and Gergeley (1975). Nonlinear least-squares analysis was performed with a program described previously (Harmon et al., 1984).

Model Describing the Linkage between Ca^{2+} and TFP Binding. (A) General. The Adair equation will appear often in these derivations; defining:

$$F(\mathrm{L},n) = \sum_{i=1}^{n} \frac{n!}{(n-i)!i!} [\mathrm{L}]^i \prod_{j=1}^{i} K_j$$

where L represents any ligand, n is the number of ligand binding sites on the protein, and K is the appropriate binding constant. The Adair equation for binding of a ligand to a protein is then

$$\frac{[\mathrm{L}]_{\mathrm{bound}}}{[\mathrm{protein}]_{\mathrm{TOT}}} = \frac{[\mathrm{L}]\, \mathrm{d}F(\mathrm{L},n)}{F(\mathrm{L},n)}$$

where dF is the derivative of F with respect to ligand concentration and TOT denotes the total concentration.

In the following derivations, Ca^{2+}-binding constants are lower-case and TFP-binding constants are upper-case.

(B) Troponin C. The conservation equation for Tn C when both Ca^{2+} and TFP are bound may be stated as

$$[\text{Tn C}]_{\text{TOT}} = [\text{Tn C}] + [\text{Tn C}]_{\text{Ca,TOT}} + [\text{Tn C}]_{\text{Ca,TFP,TOT}} \quad (1)$$

i.e., the total concentration of Tn C is equal to the sum of concentrations of free, uncomplexed Tn C and the total concentrations of the Ca^{2+}-bound forms and those having both Ca^{2+} and TFP bound, respectively. Implicit in this treatment is the assumption that TFP binding in the absence of Ca^{2+} is negligible; at the highest TFP concentration used in these experiments (33.6 μM, see Figure 9), less than 10% of the binding observed would occur in the absence of Ca^{2+} (see Figure 7). Thus, this assumption is reasonably accurate and would not influence the conclusions reached. Since Ca^{2+} binding in the absence of TFP is to four (i = 1, 2, 3, and 4) independent sites (Potter & Gergeley, 1975)

$$[\text{Tn C}] + [\text{Tn C}]_{\text{Ca,TOT}} = P[\text{Tn C}] \quad (2)$$

where $P = \prod_{i=1}^{4}(1 + k_i[Ca^{2+}])$.

Letting T* symbolize the particular Ca^{2+}-bound form or forms of Tn C that bind TFP, it can be shown that

$$[\text{T}^*] = \beta[\text{Tn C}] \quad (3)$$

where β is the appropriate term or sum of terms of the expansion of

$$\prod_{i=1}^{4}(1 + k_i[Ca^{2+}])$$

e.g., the concentration of Tn C having all four Ca^{2+}-binding sites filled is given by $\beta = k_1k_2k_3k_4[Ca^{2+}]^4$, and that for Tn C with either three or four Ca^{2+} bound is $\beta = (k_3 + k_4)k_1k_2[Ca^{2+}]^3 + k_1k_2k_3k_4[Ca^{2+}]^4$.

In the presence of 1 mM Ca^{2+}, TFP binding is described by the Adair equation for four binding sites (see Figure 8). Thus

$$[\text{Tn C}]_{\text{Ca,TFP,TOT}} = D[\text{T}^*] \quad (4)$$

where $D = F(\text{TFP},4) - 1$.

Finally

$$[\text{TFP}]_{\text{bound}} = N[\text{T}^*] = \beta N[\text{Tn C}] \quad (5)$$

where $N = [\text{TFP}]\, dF(\text{TFP},4)$.

Combining eq 1–4 yields

$$[\text{Tn C}]_{\text{TOT}} = P[\text{Tn C}] + D[\text{T}^*] = (P + \beta D)[\text{Tn C}] \quad (6)$$

Combining eq 5 and 6 yields the final binding equation:

$$r = \frac{[\text{TFP}]_{\text{bound}}}{[\text{Tn C}]_{\text{TOT}}} = \frac{\beta N[\text{TnC}]}{(P + \beta D)[\text{Tn C}]} = \frac{\beta N}{P + \beta D} \quad (7)$$

Notice that, if Ca^{2+} were absent, $\beta = 0$ and no TFP binding would occur and that, if all the Tn C was in the T* form, $\beta = P$ and eq 7 reduces to $r = N/(1 + D)$, the four-site Adair equation for TFP binding.

(*C*) *Calmodulin.* The linkage between Ca^{2+} and TFP binding to CaM was modeled as above with the following exceptions:

Since Ca^{2+} binding to CaM is adequately described by the Adair equation (Crouch & Klee, 1980) and so is TFP binding (see below), the linkage equation derived above for Tn C can be modified as follows: $P = F(Ca^{2+},4)$ and β = the ith term from the expansion of $F(Ca^{2+},4)$, where i is the number Ca^{2+} bound; e.g., for the two Ca^{2+} bound form of CaM $\beta = 6k_1k_2[Ca^{2+}]^2$, and for the free Ca^{2+} bound form of CaM $\beta = 4k_1k_2k_3[Ca^{2+}]^3$.

For TFP binding, the data were best fit by the Scatchard equation (see Results); however, the Adair equation reduces to an equation that is just an association constant form of the Scatchard equation when $K_1 = K_2 = \ldots = K_n$. Thus, we let $K_1 = K_2 = K_3 = K_4 = K_{\text{TFP}}$, $N = [\text{TFP}]\, dF(\text{TFP},4)$, and $D = F(\text{TFP},4) - 1$, and the final linkage equation is then

$$r = \frac{[\text{TFP}]_{\text{bound}}}{[\text{CaM}]_{\text{TOT}}} = \frac{\beta N}{P + \beta D} \quad (8)$$

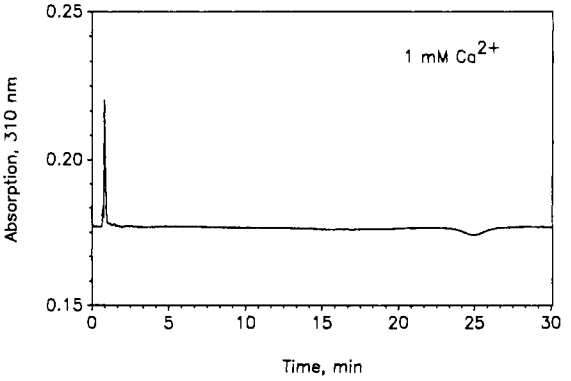

FIGURE 1: TFP binding to Tn C in Ca^{2+}. The 4.6 × 100 mm Macrosphere GPC-60 column was equilibrated at 1 mL/min in 50 mM imidazole, 150 mM KCl, 1 mM $CaCl_2$, and 48 μM TFP, pH 7. At zero time, 10 μL of a 60 μM solution of Tn C prepared in the same buffer was injected.

To model the Ca^{2+} dependency of TFP binding (Figures 6 and 9), eq 7 (for Tn C) or eq 8 (for CaM) was entered into a Lotus 123 spreadsheet along with Ca^{2+} concentrations over the range investigated. Different assumptions were made about which Ca^{2+}-bound form of each protein binds TFP, the appropriate β and P were inserted into the spreadsheet, and their Ca^{2+} dependence was calculated. Initially, the constants used to calculated β and P for Tn C were the Ca^{2+}-binding constants reported by Potter and Gergely (1975); i.e., $k_1 = k_2 = 2.1 \times 10^7$ and $k_3 = k_4 = 3.2 \times 10^5$. For the figures, the value for $k_3 = k_4 = 2.8 \times 10^5$ obtained from the fit of our data was used. For CaM, the Ca^{2+}-binding constants of Crouch and Klee (1980) were used. N and D were calculated in the spreadsheet for the concentrations of TFP used in the experiments from the constants for TFP binding in the presence of 1 mM Ca^{2+} presented under Results. The spreadsheet was then used to prepare graphs similar to those shown in the figures to allow rapid comparison of the fits of various assumptions to the data obtained.

Results

Assay Development. In developing the binding assay, both CaM and Tn C were used and gave similar results. In general, only the results obtained with Tn C will be described to simplify the discussion; however, unless otherwise stated, CaM would give similar results.

A suitable gel filtration column was needed for the binding assay. Initially, several different columns were tried and found unsuitable because they bound and retained excessive amounts of TFP and failed to equilibrate rapidly. These included the Bio-Sil TSK-125, the Rogel P, and the Synchropak GPC-60 columns. Finally, the Macrosphere GPC-60 column was found to equilibrate completely in less than 30 min with 10 μM TFP at 1 mL/min (data not shown). The Macrosphere column was used for all further experiments. Ideally, such a column should equilibrate after a few column volumes (~1.7 mL for the 4.6 × 100 mm column); that about 18 column volumes was required for equilibration suggests that this column also binds some of the drug applied to it.

Figure 1 shows the result of injecting Tn C onto the equilibrated column. The peak eluting at 0.8 min represents

Table I: Comparison of Equilibrium Dialysis and HPLC Methods

[TFP] (μM)	$[TFP]_{bound}/[Tn\ C]$	
	equilibrium dialysis	HPLC
0	0	0
3.6	0.45 ± 0.06	0.40 ± 0.04
22.7	2.88 ± 0.02	3.28 ± 0.09
61.1	3.78 ± 0.02	3.50 ± 0.17

TFP bound to Tn C, and the broad base-line trough eluting at 25 min represents the amount of TFP removed from the mobile phase by Tn C. The areas of the peak and trough were measured under several different drug concentrations and were found to be the same within 1–5% in the various experiments with either protein. Since both areas represent the amount of drug bound by protein, the close agreement shows that the detected absorbance properties of the complex must be nearly identical with that of uncomplexed TFP and the chromatography experiment is accurately measuring drug binding. Drug binding was monitored at TFP's absorption maximum at 310 nm where there is little interfering protein absorption. The molar absorptivity at this wavelength was measured as described previously (Jarrett, 1984) to be 3652 ± 96 cm^{-1} M^{-1}.

Initially, two different injection protocols were compared: either Tn C was mixed with the same concentration of TFP as the mobile phase, or Tn C that did not contain TFP was injected. The areas for the peak were the same in either case. Thus, Tn C is able to equilibrate with TFP during the transit time through the column (~0.8 min for Tn C). To calibrate protein recovery from the column, three injections of CaM were made through the column detecting at 276 nm. The column was then replaced by a zero dead volume union, and three more CaM injections were made. The peak areas for the two experiments were found to be the same within 1% and were not statistically different. Thus, all the protein injected onto the column is recovered in the effluent. In another experiment, the column was equilibrated in 50 μM TFP, and three injections were made while monitoring at 310 nm. In one case, the injections were spaced 30 min apart, and in another case, the injections occurred at 4-min intervals. It was found that the amount of drug binding measured under the two conditions was the same, indicating that it was not necessary to allow the trough from one injection to elute before another injection could be made. Since both protocols gave the same results and it requires less time to make three closely spaced injections, this latter protocol was chosen for use in the automated method.

An automated method was developed that allows the determination of drug binding in triplicate at eight different TFP concentrations with typically 270 μg of either protein in about 10 h without an operator's attention. This HPLC method was next compared to equilibrium dialysis, and the results for Tn C are presented in Table I. In this experiment, the amount of Tn C used for dialysis at a single TFP concentration was approximately the same as the amount used for the entire automated HPLC experiment. Because such greater amounts were required, binding was assayed by dialysis at only four TFP concentrations. Clearly, results obtained with the two methods agree quite well. The largest differences found were at 22.7 μM, a concentration close to the apparent dissociation constant for binding (see below). Since the amount bound varies most rapidly with TFP concentrations near the dissociation constant, this is where small differences in TFP concentration can have the largest effect on binding and where the greatest variation is to be expected. The HPLC assay and equilibrium dialysis also gave very similar results for CaM (data not shown). Thus, the HPLC method is about as accurate as equilibrium dialysis, which required 14 times more protein.

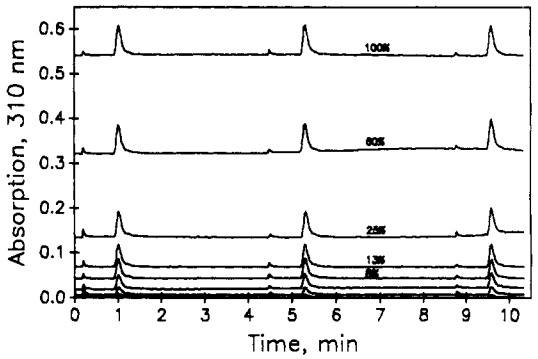

FIGURE 2: TFP binding to calmodulin in the presence of 1 mM calcium was measured by the HPLC binding assay. The automated HPLC binding assay described was used with the 4.6 × 100 mm Macrosphere GPC-60 column. A narrow time window around each set of injections is presented for clarity. Unless stated otherwise, for all HPLC studies of CaM, buffer A was 50 mM MES, 150 mM KCl, and 1 mM $CaCl_2$, pH 6.5, and buffer B was the same as buffer A except that it contained TFP, in this case 148 μM. 10 μL of 60 μM CaM in buffer A was the sample injected. For each percentage of buffer B (shown above upper chromatograms), the time at which the first injection occurred is referred to as zero time, and the elution profile for the next 10 min is shown. From top to bottom, the chromatograms are for 100, 60, 25, 13, 8, 4, 2, and 0% buffer B, respectively. The concentration of TFP in the mobile phase was obtained from the base-line absorption at 310 nm and was 148.4, 89.3, 37.3, 18.7, 11.76, 5.56, 1.72, and 0 μM TFP, respectively.

The HPLC column was found to equilibrate most readily with TFP at lower pH values. For this reason, most studies of CaM were carried out at pH 6.5. However, for Tn C which has a much higher affinity for Ca^{2+} (Potter & Gergely, 1975) the higher pH of 7.0 was used primarily so that EGTA would be a more effective chelator when used. However, cross comparisons with each protein indicated that pH over this narrow range has little effect on TFP binding (data not shown). Since the binding of TFP to each protein was different, we will discuss CaM and Tn C separately below.

Calmodulin. Figure 2 shows a typical HPLC-binding experiment in buffers containing 1 mM Ca^{2+}. The HPLC column was equilibrated in different percentages of buffer B that contained 148 μM TFP, and triplicate injections of 60 μM CaM were made. Detection of TFP at 310 nm and integration of peak area give the amount of TFP bound to the injected CaM. This figure shows the reproducibility of replicate injections and the stable base lines encountered. The actual concentration of TFP at which a peak elutes is determined for each peak from the base-line absorption of the equilibrated column, and so the method does not depend directly on the accuracy of the HPLC pumps; however, we found the pumps to be accurate to within about 2% in all cases. CaM gives similar peak shape and symmetry at all TFP concentrations up to ~150 μM (the highest concentration tested). Similar experiments performed in the absence of Ca^{2+} show no significant TFP binding over this concentration range (data not shown but see below).

Figure 3 shows the combined TFP-binding data of six different experiments in 1 mM Ca^{2+}. The data were fit to various binding equations (Scatchard, Hill, and Adair for n = 1–5), and the best fit was found to the Scatchard equation with n = 4.2 ± 0.2 and K_d = 5.8 ± 0.9 μM; the line shown on the figure was obtained with this equation and the derived values. The Adair equation that best fit the data was the one for four sites, and the association constants for each of the four sites were not significantly different; the inverse fourth root

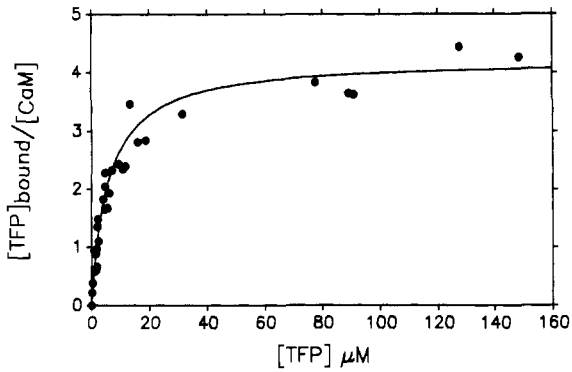

FIGURE 3: Concentration dependency of TFP binding to CaM in 1 mM Ca^{2+}. The automated method was used with the buffers that contained 1 mM Ca^{2+} as described for Figure 2, and the data from six different experiments have been combined. Each point represents the mean of three determinations, and the area of CaM injected in the absence of TFP has been subtracted from the other data. The concentration of TFP was determined independently for each point from the base-line absorption at 310 nm immediately before the peak eluted. The line shown is for the Scatchard equation with $n = 4.2$ and $K_d = 5.8$ μM.

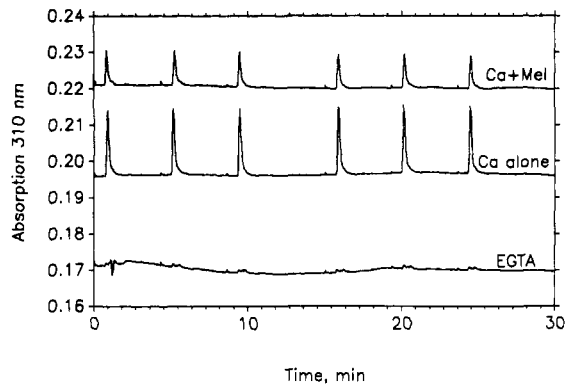

FIGURE 4: Effect of EGTA, Ca^{2+}, and melittin on TFP binding to calmodulin. The mobile phase and the CaM injected throughout contained 49.5 μM TFP, 150 mM KCl, and 50 mM MES, pH 6.5. As denoted on the figure, where present, EGTA or Ca^{2+} was 1 mM in the injected CaM and in the column mobile phase; where present, melittin was 30 μM in the sample and 2 μM in the mobile phase. The sample was 30 μM CaM throughout, and six automated 10-μL injections are shown for each chromatogram. The chromatograms are shown to the same scale but have been offset by 0, 0.02, or 0.04 absorbancy from the bottom to the top curve, respectively.

of the product of the four Adair constants (Harmon et al., 1984) was 4.7 μM in agreement with the K_d obtained from the fit to the Scatchard equation. The Hill coefficient was 0.82. Taken together, these observations are consistent with noncooperative, independent binding of 4 TFP/CaM.

Figure 4 shows the TFP binding encountered in EGTA, Ca^{2+}, and Ca^{2+} + melittin. For these experiments, the column was equilibrated in 49.5 μM TFP. The peak areas correspond to 0.15 ± 0.02, 4.23 ± .09, and 2.18 ± 0.12 equiv of TFP bound for the three conditions, respectively. When EGTA is present, very small peaks are observed, indicating little if any TFP binding. The peaks observed under these conditions are only slightly larger (but not significantly so) than those obtained when the same amount of CaM is injected in the absence of TFP (see Figure 2) and may not represent true TFP binding. When Ca^{2+} is present, 4.2 TFP is bound, and the addition of equimolar melittin to the sample and 2 μM melittin to the mobile phase reduces TFP binding to about half this amount. Since melittin binds to CaM with nanomolar affinity (Maullet & Cox, 1983), under these conditions all CaM should be bound to melittin, and apparently, half of the TFP-binding sites no longer bind the drug when melittin is bound.

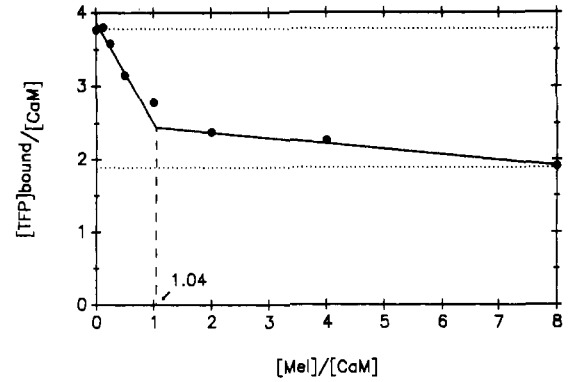

FIGURE 5: Titration of CaM with melittin shows that a single melittin displaces two TFP. The column was equilibrated in 49.8 μM TFP, 20 nM melittin, and 1 mM Ca^{2+} in buffer A described for Figure 1; the column was maintained isocratic in this buffer throughout. The samples were prepared to contain 60 μM CaM and the proportional amount of melittin denoted in the figure made up in the same solution as the mobile phase. Triplicate injections 4 min apart of each of the eight samples were then made with 35 min between samples. The solid lines shown are the result of linear least squares of the four leftmost or three rightmost data, respectively, and their point of intersection is shown by the vertical dashed line. The two horizontal lines show the predicted TFP binding calculated from the Scatchard equation for $n = 4$ (upper line) or $n = 2$ (lower) TFP-binding sites assuming $K_d = 5.8$ μM.

Since the concentration of CaM injected is 30–60 μM in these experiments while the affinity of melittin for CaM is in the nanomolar range, a titration of the melittin-binding sites on CaM which affect TFP binding is feasible. Such an experiment is shown in Figure 5. As melittin is added, CaM binds less TFP, and the data reveal how much melittin is required to cause the effect. In this experiment, a straight line connecting the data at low [melittin]/[CaM] ratios and the one connecting the data at high ratios should intersect at the ratio of melittin/CaM that causes the effect on TFP binding. As the figure shows, the binding of one melittin (intersection at [melittin]/[CaM] = 1.04) causes the observed effect on TFP binding. This analysis of the data is crude but is sufficient since Maulet and Cox (1983) have already shown that only one melittin binds to CaM in the presence of Ca^{2+}. Also shown on the figure are two horizontal lines which show the calculated TFP binding that should be observed at this TFP concentration if either four or two sites on CaM are binding TFP. From this experiment, one can conclude that CaM binds about four TFP in the absence of melittin and that, as a single melittin binds, it displaces two TFP and two TFP remain bound.

Figure 6 shows the results of an experiment to learn how many Ca^{2+} must be bound by CaM for TFP binding to occur. Since Ca^{2+} binding is required for TFP binding, the two binding equilibria are linked functions (Wyman, 1964), and the Ca^{2+} dependence of TFP binding can be used to discover how many Ca^{2+} must be bound to CaM for TFP binding to occur. The solid-line curves show the predicted behavior if TFP binds to the form of CaM that has one, two, three, or four Ca^{2+} bound, respectively. All of these curves were calculated for 47.6 μM TFP, the highest concentration tested. Clearly, the model for TFP binding to the three Ca^{2+} bound form best fits the data (closed circles). The dotted lines show the results of using this model for the three Ca^{2+} bound form of CaM to predict the behavior for the two lower TFP concentrations. Clearly, the model adequately fits the data over a range of TFP concentrations.

The Ca^{2+}-binding constants used for the calculated curves were those reported by Crouch and Klee (1980), and the TFP-binding constants used were obtained from the data in

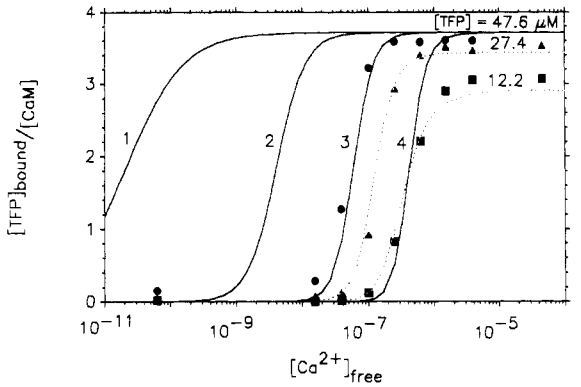

FIGURE 6: Calculated dependence of TFP binding on the concentration of free Ca^{2+}. The HPLC was equilibrated at 1 mL/min in buffer A (100 mM KCl, 10 mM imidazole, 10 mM EGTA, pH 7.00). Buffer B was the same as buffer A except that in addition to the EGTA and TFP, it also contained 10 mM $CaCl_2$. In this and the related experiment in Figure 9, the pH of the buffers was adjusted to within 0.01 unit since the concentration of free Ca^{2+} is highly dependent upon pH. The HPLC was programmed to hold at 0, 7, 16, 33, 55, 75, 88, 95, and 100% buffer B for 30 min and at 20 min after beginning a new percentage to make three 10-μL injections of 60 μM CaM dissolved in buffer A. The results shown are the averages for the three injections. The concentration of free, uncomplexed Ca^{2+} was calculated (Perrin & Sayce, 1967), taking into account the 3 μM measured Ca^{2+} contamination of the buffers, and is shown on the abscissa. The results of three separate experiments at 47.6 (circles), 27.4 (triangles), or 12.2 μM TFP (squares), respectively, are shown. The solid line curves were calculated with eq 8 for a [TFP] = 46.7 μM to correspond to the highest concentration used. For TFP binding, it was assumed that the following dissociation constants apply: K_1 = 3.8 μM, K_2 = 10.9 μM, K_3 = 3.6 μM, and K_4 = 3.2 μM. These values were obtained from the Adair equation fit of the data in Figure 3. Virtually indistinguishable curves would be obtained by using $K_1 = K_2 = K_3 = K_4 = K_{TFP} = 4.7\ \mu M = (K_1K_2K_3K_4)^{1/4}$. For Ca^{2+} binding, the values for the four constants used were those reported by Crouch and Klee (1980). The curves are labeled with the number of Ca^{2+} assumed to be bound by CaM when TFP binds; i.e., curve 1 results from the equation for TFP binding to CaM·Ca, curve 2 results from that for TFP binding to CaM·Ca_2, etc. The dotted lines show the predicted behavior for the two lower TFP concentrations, assuming that TFP binds to CaM·Ca_3 (i.e., $\beta = 4k_1k_2k_3[Ca^{2+}]^3$); this is the same as solid curve 3 except for the lower TFP concentration used for the calculations.

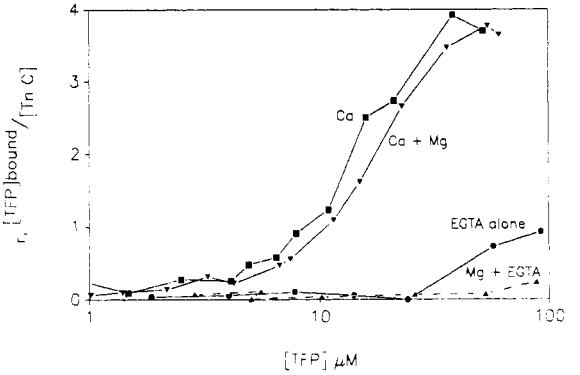

FIGURE 7: Concentration dependency of TFP binding to Tn C in the presence and absence of Ca^{2+} and Mg^{2+}. The automated method was used with buffers that contained 1 mM Ca^{2+}, 1 mM Ca^{2+}/3 mM Mg^{2+}, 10 mM EGTA, or 10 mM EGTA/4.1 mM Mg^{2+} as indicated. For Tn C unless otherwise stated, HPLC assay buffer A was 50 mM imidazole and 150 mM KCl, pH 7, with other additions as noted, and buffer B was the same as buffer A except that it contained TFP. The higher pH used with Tn C was necessary to make the EGTA present in some experiments a more effective Ca^{2+} chelator. Each point shown represents the mean of three determinations with the exception of the TFP absent data, which are the mean of six determinations and have been subtracted from the other data. The concentration of TFP was determined independently for each point from the base-line absorption at 310 nm immediately before the peak eluted.

Figure 3 (at 1 mM Ca^{2+}). When the data for all TFP concentrations were fit to the equation for the three Ca^{2+} bound form of CaM, the following intrinsic binding constants were obtained: K_{TFP} = 4.5 μM (compared to 5.8 μM in Figure 2) and, for Ca^{2+}, k_1 = 3.3 μM, k_2 = 0.5 μM, and k_3 = 10 μM. These last three values are similar to those reported by Crouch and Klee (1980), who gave values of 3.3, 1.2, and 8.3 μM, respectively, under similar conditions, and also agree reasonably well with values reported by Haiech et al. (1981). The fitting process demonstrated that the data in Figure 6 do not contain information about the fourth Ca^{2+}-binding constant and so this was set to 22 μM as reported by Crouch and Klee (1980) during the fitting process.

The data in Figure 6 also show the effect of TFP on the Ca^{2+} affinity of CaM. As predicted on the basis of the linkage function, the presence of TFP increases the affinity of CaM for Ca^{2+}. On the basis of the binding data of Crouch and Klee (1980), half-maximal Ca^{2+} binding (in the absence of TFP) would occur at about 5.2 μM Ca^{2+}. As shown in Figure 6, 46.7 μM TFP increases CaM's Ca^{2+} affinity to about 0.08 μM, and other, lower TFP concentrations cause a smaller increase in Ca^{2+} affinity.

Troponin C. The concentration dependency of TFP binding to Tn C showed an interesting difference from the results obtained with CaM. In experiments similar to that shown in Figure 2, at TFP concentrations above ~60 μM the Tn C peak begins to broaden significantly, and at concentrations above ~100 μM the peaks become so broad they become difficult to detect. Thus, TFP has some effect on Tn C's chromatographic behavior (data not shown but submitted for review). The cause of this peak broadening is not known, but several further observations may be relevant. In the presence of EGTA or Mg + EGTA, broadening was also observed, but it typically occurred only at TFP concentration above 100 μM while in the presence of Ca^{2+} or Ca^{2+} + Mg^{2+} it occurred above ~60 μM. The same peak broadening did not occur in similar experiments with CaM even at TFP concentrations approaching 150 μM (Figure 2). Thus, the phenomenon appears to be peculiar to Tn C. Peak width in gel filtration chromatography is sensitive to the aggregation state, overall shape, and folding of proteins. Thus, the broadening seen with Tn C may indicate some change in the aggregation or conformation of Tn C in high concentrations of TFP. In the experiments presented below, only data obtained at lower TFP concentrations where peak broadening did not occur are shown.

Figure 7 illustrates TFP binding to Tn C in the presence or absence of Ca^{2+} and Mg^{2+}. Very little TFP binding occurs in 10 mM EGTA and even less in 4.1 mM Mg^{2+} plus 10 mM EGTA. Calculations (Perrin & Sayce, 1967) showed that the latter conditions would result in 3 mM uncomplexed Mg^{2+}. In the presence of 1 mM Ca^{2+} with or without 3 mM Mg^{2+}, TFP binding approaches 4 equiv at higher TFP concentrations. In either case, half-maximal binding occurs at ~16 μM.

The TFP-binding data in Ca^{2+}/Mg^{2+} gave a Hill coefficient of 1.7, indicating positive cooperativity in agreement with Levin and Weiss (1978). Our Hill coefficient is somewhat lower than that previously reported (Levin & Weiss, 1978); however, our data also suggest a break in the data occurring at about 10 μM with the data at higher concentrations being better fit by a larger Hill coefficient (i.e., a steeper slope). Thus, while the data suggest positive cooperativity, they also suggest that TFP binding is rather complicated, and the binding was further analyzed.

The TFP binding measured in the presence of Ca^{2+}/Mg^{2+} was fit by nonlinear least squares (Harmon et al., 1984) to

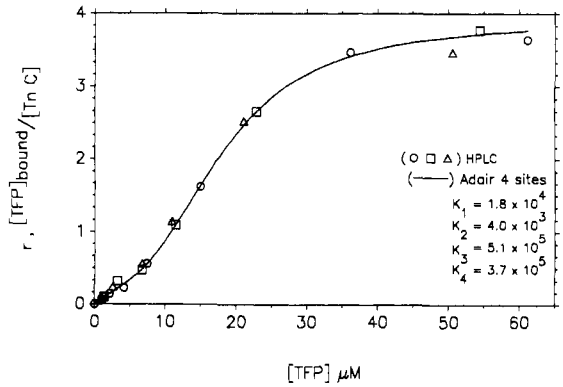

FIGURE 8: Adair equation for four binding site fits the Tn C binding data. The Adair equation for four sites was fit to the data for TFP binding in 1 mM Ca^{2+} plus 3 mM Mg^{2+}, and the goodness of fit is shown in the figure. Data from three different experiments (○, △, □) are shown. The line shown was calculated from the Adair equation and the constants shown.

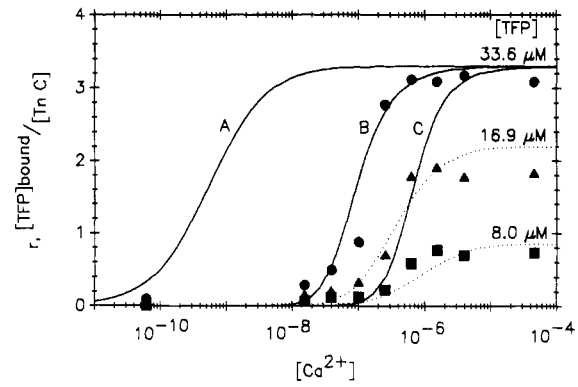

FIGURE 9: Calculated dependence of TFP binding on the concentration of free Ca^{2+}. The HPLC method and buffer compositions were the same as in Figure 6 except for the TFP concentration. The results of three separate experiments at 33.6 (circles), 16.9 (triangles), and 8 μM (squares) are shown. The curves were calculated with eq 7 for 33.6 μM TFP to correspond to the highest concentration used. Different assumptions were made about the Ca^{2+} binding that influences TFP binding, and these assuptions gave rise to the curves shown. (A) TFP binding requiring only Ca^{2+} binding to the two high-affinity Ca^{2+}–Mg^{2+} sites on Tn C; (B) TFP binding requiring Ca^{2+} binding to either of the low-affinity, Ca^{2+}-specific sites; (C) TFP binding requiring that both low-affinity Ca^{2+}-specific sites bind Ca^{2+}. The dotted-line curves show the results of applying the same equation as that used for curve B [i.e., $\beta = (k_3 + k_4)k_1k_2[Ca^{2+}]^3 + k_1k_2k_3k_4[Ca^{2+}]^4$] to the two lower TFP concentrations. The constants for TFP binding used were the Adair constants for TFP binding in 1 mM Ca^{2+} given in the text; for Ca^{2+} binding, $k_1 = k_2 = 2.1 \times 10^7$ given by Potter and Gergely (1975) was used along with $k_3 = k_4 = 2.8 \times 10^5$ derived in our studies. Using Potter and Gergely's value for k_3 and k_4 would have negligible effect.

various models using the resulting χ^2 to judge how well the model fit the data. The best fit was to the Adair equation for four binding sites. The Scatchard equation gave a 25-fold higher χ^2, indicating that a simple noncooperative model does not fit the data. The Hill equation gave a somewhat better fit than the Scatchard, but the best fit was obtained with the Adair equation for four binding sites. The Adair constants obtained and the fit of the equation to the data for 1 mM Ca^{2+}/3 mM $MgCl_2$ are shown in Figure 8. For similar binding in the absence of Mg^{2+} (data not shown), the fit gave $K_1 = 2.5 \times 10^4$, $K_2 = 6.6 \times 10^3$, $K_3 = 5.8 \times 10^5$, and $K_4 = 2 \times 10^5$ M^{-1}. The standard deviation for all the fitted constants was less than 5% of the values given. That the constants are similar in the presence or absence of Mg^{2+} suggests little influence of Mg^{2+} on TFP binding. The Adair constants obtained show the complicated cooperativity of TFP binding to Tn C. For such constants, the Adair equation indicates no cooperativity when $K_1 = K_2 = K_3 = K_4$, negative cooperativity when $K_1 > K_2 > K_3 > K_4$, and positive cooperativity when $K_1 < K_2 < K_3 < K_4$. The values obtained indicate that TFP is bound by a combination of negative and positive cooperative binding events since they may be characterized as $K_1 > K_2 < K_3 \geq K_4$.

Figure 9 shows the result of an investigation to learn which Ca^{2+}-bound form of Tn C binds TFP. TFP binding to various Ca^{2+}-bound forms of Tn C can be distinguished. As was done above for CaM, the solid line curve shows the predicted behavior at the highest TFP concentration (33.6 μM) if TFP binds to various Ca^{2+}-bound forms of Tn C. TFP binding that requires Ca^{2+} binding to only the two high-affinity sites on Tn C (Figure 9A) would occur at over 2 orders of magnitude lower $[Ca^{2+}]$ than TFP binding requiring Ca^{2+} binding to either of the low-affinity Ca^{2+}-binding sites (Figure 9B). Clearly, the data at 33.6 μM TFP best fit this latter model (Figure 9B). TFP binding to only the $(Ca^{2+})_4$-bound form of Tn C (Figure 9C) would shift TFP binding another 0.9 pCa unit to higher Ca^{2+} concentration, and this is clearly inconsistent with the data.

The fit of the data to these models suggests it is binding of the third Ca^{2+} to a low-affinity Ca^{2+}-binding site on Tn C (Figure 9B) which is required for TFP binding. TFP binding occurs at too high a $[Ca^{2+}]$ to be accounted for by Ca^{2+} binding to only the two high-affinity Ca^{2+}-binding sites (Figure 9A) and at too low a $[Ca^{2+}]$ to be accounted for if TFP binding occurs only to the form of Tn C with all four Ca^{2+}-binding sites occupied (Figure 9C). It is most likely that the third Ca^{2+} which binds to Tn C initiates TFP binding. The equation for binding to this form of Tn C also fits the behavior observed at other, lower TFP concentrations (dotted lines).

The data also show that TFP binding induces an increase in the Ca^{2+} affinity of the two low-affinity Ca^{2+}-binding sites on Tn C. As TFP is increased from 8 to 33.6 μM, the concentration of Ca^{2+} required for half-maximal TFP binding decreases from 0.89 to 0.096 μM Ca^{2+}. Thus, TFP increases the affinity of Tn C for Ca^{2+}. TFP also increases the Ca^{2+} sensitivity of myofilament contraction (Herzig et al., 1987) as would be expected from the data in Figure 9; thus, these data are consistent with previous reports. The data were fit to the equation (for TFP binding to Tn C having either of the low-affinity Ca^{2+}-binding sites occupied) by nonlinear least squares (Harmon et al., 1984). The resulting constants for TFP binding were virtually identical with those already given for TFP binding in 1 mM Ca^{2+}. The fit of the data also gives the intrinsic Ca^{2+}-binding constant that affects TFP binding, and this derived value was 2.8×10^5 M^{-1}. This value is in excellent agreement with the value of 3.2×10^5 M^{-1} measured by Potter and Gergely (1975) for the two low-affinity, Ca^{2+}-specific sites on Tn C in the absence of TFP.

Discussion

The HPLC method developed to study TFP binding represents a natural extension of the low-pressure binding method first described by Hummel and Dreyer (1962) to modern chromatographs. Not all gel filtration media are equally suited for these binding studies, the Macrosphere GPC-60 being the only column that could be equilibrated with TFP fairly rapidly. Even this column retained significant amounts of TFP during equilibration, and this was probably the reason the trough of bound drug eluted at 25 min (Figure 1) rather than at the column included-volume retention time of 1.7 min measured with tryptophan or 2-mercaptoethanol. This retention of TFP by the column would be troublesome if it perturbed the free

concentration of TFP in the mobile phase, but this is apparently not the case since equilibrium between applied and eluting mobile phases is obtained and the method gives results similar to those obtained by equilibrium dialysis (Table I) and yielded determinations of the affinity of Ca^{2+}-binding sites on both proteins which agree well with previous reports. Indeed, the TFP retained by the column may act beneficially to buffer the free concentration of TFP during the experiment.

Since each protein gave somewhat different results, it is appropriate to discuss them separately:

Calmodulin. The results may be summarized as follows: In the presence of Ca^{2+}, CaM binds about 4 equiv of TFP with an affinity in the range of 4.5–5.8 μM, and binding is apparently noncooperative. Very little if any TFP is bound in the absence of Ca^{2+} under the conditions used. A single melittin competes with two of these TFP for binding to CaM. Finally, three Ca^{2+} must be bound by CaM if it is to bind TFP.

The number and affinity of TFP-binding sites on CaM found in this study differ from those of Levin and Weiss (1978). We find very little Ca^{2+}-independent binding of TFP (not 27 sites) and four Ca^{2+}-dependent sites (rather than two). This probably has to do with the ionic strength of the buffers used. In preliminary experiments with buffers of less than 50 mM total salts, CaM bound much greater amounts of TFP while, at all salt concentrations above 50 mM, we consistently found a maximum of 4 equiv of TFP bound (data not shown). Probably at low ionic strengths the cation TFP can charge pair with the very acidic protein CaM. Thus, the low ionic strength (5 mM) used in earlier studies (Levin & Weiss, 1978) may have contributed to the large amount of low-affinity TFP-binding observed. It is interesting to note that 27 low-affinity binding sites observed in these studies are close to the net negative charge expected at neutral pH on the basis of CaM's sequence (Watterson et al., 1980). Consistent with this interpretation, at higher ionic strengths such as those used here (100–150 mM KCl) and in another study (Marshak et al., 1985) much less phenothiazine binding is observed, and it is highly Ca^{2+} dependent. While our results more closely resemble those of Marshak et al., we find that four phenothiazines bind rather than five. The reason for this difference is unknown.

The results with melittin show that there are two different classes of bound TFP: two of the TFP that bind are displayed by melittin binding, and two others are not. The significance of this result lies in the likelihood that melittin is an analogue for the CaM-binding regions of at least some enzymes.

The CaM-binding sequences from several enzymes have been identified including those derived from skeletal and smooth muscle myosin kinase (Blumenthal et al., 1985; Edelman et al., 1985; Lukas et al., 1986) and the more recently elucidated structure of the putative CaM-binding region of Ca^{2+}-transport ATPase (James et al., 1988). These CaM-binding regions are notable in that they have a calculated propensity for α-helical structure and contain two clusters of cationic amino acids adjacent to hydrophobic regions of structure. Melittin also has this same cationic-adjacent-to-hydrophobic motif, has a propensity for alpha α-helical structure, and is also bound by CaM with high affinity ($\sim$1 nM) (Maulet & Cox, 1983; Anderson & Malencik, 1986). A comparison of the structures of melittin and the CaM-binding regions of these three enzymes demonstrates that melittin shows as much similarity to any one of these enzyme-derived peptides as they do to one another. Furthermore, both ends of CaM's structure are involved in complex formation with either enzymes or melittin, and many of the same residues of CaM are known to participate in both interactions (Jackson et al., 1986; Steiner et al., 1986; Klevit et al., 1985). The close structural similarity of melittin and the CaM-binding region of enzymes is also suggested by the observation that antibodies raised against melittin bind to CaM-activated enzymes and can displace CaM (Kaetzel & Dedman, 1987). Melittin is thus an analogue of the CaM-binding regions of at least some enzymes.

TFP is a hydrophobic cation, and its similarity in chemical properties with the hydrophobic, cationic CaM-binding regions of enzymes has been suggested to account for the antagonism of enzyme activation by TFP (LaPorte et al., 1980; Hidaka et al., 1980). On the basis of this model, presumably TFP, enzymes, and antagonist peptides all bind to similar sites on CaM. Results with β-endorphin, another CaM antagonist peptide, and with two CaM-activated enzymes support this argument. Binding of TFP, β-endorphin (Giedroc et al., 1985), calcineurin (Winkler et al., 1987), or myosin kinase (Jackson et al., 1986) protects Lys^{148} and Lys^{75} of CaM from acetylation with acetic anhydride.

However, here we show only two of the TFP bound by CaM are in competition with melittin (and presumably enzymes with melittin-like CaM-binding sites) while two other TFP are not involved.

TFP binding requires that three Ca^{2+} must be bound by CaM. In this regard, it is interesting to note that three Ca^{2+} must also be bound for the activation of at least some target enzymes (Crouch & Klee, 1980). Furthermore, TFP binding increases CaM's affinity for Ca^{2+} (Figure 6) just as enzyme binding (Olwin & Storm, 1985) or melittin binding (Maulet & Cox, 1983) also increases CaM's affinity for Ca^{2+}. Thus, there are many similarities between enzyme, peptide, and TFP binding which support the argument that the competition between these various ligands for CaM is due to all being bound by similar regions of CaM and involving similar forces, i.e., cationic amphipathic ligands bound by anionic amphipathic sites on CaM.

The location of the four TFP-binding sites was further investigated by docking a molecular model of N^{10}-(3-aminopropyl)-2-(trifluoromethyl)phenothiazine to the unrefined X-ray crystal structure of CaM (Kretsinger et al., 1986) with the computer. The CaM sequence is composed of two homologous half-sequences that probably arose by a process of gene duplication (Watterson et al., 1980). As previously described, there is a hydrophobic cup at the COOH-terminal end of CaM bounded by Lys^{148}, Met^{109}, and Met^{144} and a similar hydrophobic cup at the NH_2-terminal end bounded by the residues at homologous sequence positions (Lys^{75}, Met^{36}, and Met^{71}, respectively) (Faust et al., 1987; Kretsinger et al., 1986). Each hydrophobic cup structure has nearby clusters of acidic residues that could charge pair with the cationic phenothiazine drugs, and we propose that each of these regions binds a single phenothiazine. This would account for two of the TFP that are bound, and we further propose that it is these two TFP which are displaced by melittin. The closest approach of these hydrophobic cups to one another is about 12–15 Å, which is a short enough distance to allow melittin and other peptide antagonists to bind to both cup structures simultaneously. Such a placement of TFP would be close enough to the two Lys mentioned to explain their affinity labeling by a TFP analogue (Faust et al., 1987) and would account for the protection of these residues from acetylation by TFP, an antagonist peptide (Giedroc et al., 1985), and upon enzyme binding (Winkler et al., 1987; Jackson et al., 1986). The location of the other two TFP-binding sites is less clear. At

the floor of this hydrophobic cup structure is what appears to be a herringbone stack (i.e., a perpendicular ring flanked on either side by horizontal rings) of phenylalanine rings (namely, sequence positions 89, 92, and 141 and the homologous positions 16, 19, and 68). On the other side of these Phe are other hydrophobic regions bounded by Val^{142}, Ile^{85}, and Tyr^{138} at one end of CaM and Leu^{69}, Phe^{12}, and Phe^{65} at the other end. This latter site also has Lys^{21} nearby, and this may explain why this residue reacted with the TFP analogue affinity label (Faust et al., 1987) and is protected from acetylation by the binding of some enzymes (Winkler et al., 1987; Jackson et al., 1986). Thus, we suggest that phenothiazines bind on either side of the Phe stack at each end of CaM. The involvement of these Phe in binding may explain why aromatic compounds such as the phenothiazines are bound with high affinity (LaPorte et al., 1980).

Troponin C. The results may be summarized as follows: In the presence of Ca^{2+}, Tn C binds about 4 equiv of TFP with an affinity of about 16 μM, and binding shows complex cooperativity between the sites. Apparently, TFP binding is dependent on Ca^{2+} binding to the low-affinity, Ca^{2+}-specific binding sites on Tn C. Less than 1 equiv of TFP is bound in the presence of EGTA, and this is reduced to about 0.2 equiv when Mg^{2+} is included.

While it is clear that some TFP binding does occur in the presence of EGTA (Figure 7), this binding is of much lower affinity and occurs only at concentrations of TFP that caused a broadening of the peak for the eluted TFP–Tn C adduct. Inclusion of 3 mM uncomplexed Mg^{2+} reduced TFP binding, and this suggests several possible explanations for the apparent Ca^{2+}-independent binding. There are two Mg^{2+}-specific binding sites on Tn C (Potter & Gergeley, 1975), and occupancy of these sites may decrease true Ca^{2+}-independent binding of TFP. Alternatively, it can be shown that inclusion of Mg^{2+} in the EGTA-containing buffers increases the ionization of EGTA and further lowers the free concentration of the small Ca^{2+} contamination present in the buffers ($\sim$3 μM). This small contamination results in calculated (Perrin & Sayce, 1967) free concentrations of pCa = 9.21 and 10.19 in 10 mM EGTA with and without Mg^{2+}, respectively. Since high TFP concentrations increase the affinity of Tn C for Ca^{2+} (Figure 9), high TFP concentrations may allow some Ca^{2+} binding to occur even at these low Ca^{2+} concentrations. If so, the Ca^{2+} independence would only be apparent and would actually be due to the small Ca^{2+} contamination of the buffers.

Our results are in general agreement with those of Levin and Weiss (1978) but disagree in some particulars. Although these investigators did not directly address the number of TFP binding sites on Tn C, their data clearly show the binding of more than 4 equiv of TFP at the higher end of the concentration range used in our study. The reason for the higher binding in their experiment may have to do with the ionic strength used as discussed above. Alternatively, the peak broadening observed in our gel filtration experiment suggests that high TFP concentrations may alter the aggregation or conformation of Tn C. If so, the previous data (Levin & Weiss, 1978) may indicate higher TFP binding to this form of Tn C. Whatever the cause of these differences, our data clearly show that, in the concentration range of 0–60 mM TFP, a maximum of 4 equiv of TFP is bound. Half-maximal binding occurred at 16 μM in the studies presented here (Figure 9), which is similar to the 5 μM found previously (Levin & Weiss, 1978).

The number of TFP binding sites on Tn C was uncertain. Levin and Weiss (1978) did not directly address this issue although they stated that maximal binding of four was assumed for their Hill plot. ^{1}H NMR experiments have shown that Tn C and CaM's amino acid side-chain resonances are maximally affected when 2 equiv of TFP was added (Gariépy & Hodges, 1983; Dalgarno et al., 1984; Drabikowski et al., 1985; Krebs & Carafoli, 1982; Klevit et al., 1981; Reid, 1983; Reid et al., 1983). That resonances were not further changed by additional TFP may suggest that additional binding causes no measurable changes in additional side-chain resonances. Alternatively, the high concentrations of protein required in the NMR experiments required millimolar concentrations of TFP to reach 2 equiv of drug and may not be directly comparable to the binding measured here at much lower concentrations of TFP and Tn C. Over the range of 0–60 μM TFP, our data clearly show that 4 equiv of TFP is bound in the presence of Ca^{2+} (Figure 8), and these data are confirmed by equilibrium dialysis measurements under the same conditions (Table I).

The binding of TFP to these four sites shows complicated cooperativity (Figure 8). The order of the Adair constants obtained suggests that first low-affinity binding occurs at two sites which influence each other's binding in a negative way. This low-affinity binding then induces higher affinity binding at two other sites. Such binding studies do not yield information about the location or geometric relationships of the sites involved, but the symmetry of the Tn C molecule may suggest such relationships. The amino acid sequence of Tn C is composed of two homologous half-sequences (Collins et al., 1973). Thus, one would expect that half of the four sites are in each half of the protein.

The Ca^{2+} dependence of TFP binding (Figure 9) gives further information about the location of the Ca^{2+}-binding sites that influence TFP binding. The crystal structure of Tn C (Herzberg & James, 1985; Sundaralingam et al., 1985) is similar to that of CaM and shows that these two half-sequences are parts of a roughly dumbbell-shaped molecule with two globular ends, representing the NH_2- and COOH-terminal halves of the protein, connected by an α-helical shaft. The two high-affinity Ca^{2+}-binding sites are in the COOH-terminal globular end, and the binding of Ca^{2+} at these two sites is not sufficient for TFP binding. Rather, it is the third Ca^{2+} that binds at a low-affinity Ca^{2+}-specific site (Figure 9) located in the NH_2-terminal globular end (Herzberg & James, 1985; Sundaralingam et al., 1985) which allows TFP to bind. It is interesting to note that it is Ca^{2+} binding to these same low-affinity, Ca^{2+}-specific sites which also regulates the actinomyosin ATPase (Potter & Gergeley, 1975). Since it is Ca^{2+} binding in the NH_2-terminal domain which initiates TFP binding, we propose that TFP initially binds nearby and also in the NH_2-terminal end. TFP binding is highly cooperative at the third and fourth sites (Figure 8), and initial TFP binding is of low affinity (10^3–10^4 M^{-1}); but as the second TFP binds, high-affinity ($\sim 10^5$ M^{-1}) TFP-binding sites become available and bind TFP. If, as we propose, half of the four TFP-binding sites are in each half of Tn C's structure, the cooperativity observed for TFP binding suggests that the two globular ends of the molecule must interact with one another during drug binding. The helical shaft of Tn C may mediate this interaction of the two ends. However, Tn C in solution at pH values near those used may have a more flexible central helical shaft (Heidorn & Trewhella, 1988) than is suggested by the crystal structure (Herzberg & James, 1985; Sundaralingam et al., 1985) though there is some disagreement on this point (Hubbard et al., 1988). The closer approach of the globular ends proposed for the solution conformation (Heidorn &

Trewhella, 1988) would also allow the interaction between the two globular ends predicted by the TFP-binding data and our model.

Previous models of TFP binding to either Tn C or CaM (Hidaka et al., 1980; Dalgarno et al., 1984; Drabikowski et al., 1985; Krebs & Carafoli, 1982; Klevit et al., 1981; Reid, 1983a,b; Strynadka & James, 1988) have discussed the possible location of two drug-binding sites on these proteins. These models propose that TFP is bound by a lipophilic region formed by aliphatic and aromatic side chains contributed by α-helices which are also part of the "EF-hand" (Kretsinger & Nickolds, 1973) structure of Ca^{2+}-binding sites. This could account for the linkage between Ca^{2+} binding and TFP binding observed here. However, current models did not account for the binding of 4 equiv of TFP, nor did they account for the cooperativity of binding to Tn C shown here or in a previous study (Levin & Weiss, 1978).

CaM and Tn C are homologous proteins but they differ in important ways. Tn C has two recognizably different classes of Ca^{2+}-binding sites, and this makes it possible to determine that it is the third Ca^{2+} which binds (Figure 9) at a site in the NH_2-terminal half of the sequence (Herzberg & James, 1985) which is necessary for TFP binding. In the case of CaM, TFP binding also requires that three Ca^{2+} be bound, but the location of the three occupied sites is not known. Some of the differences in structure also result in TFP binding being either highly cooperative (Tn C) or noncooperative (CaM). In either case though, both proteins have similar affinities for TFP (approximately 5 and 16 μM for CaM and Tn C, respectively) and the same number of TFP-binding sites. How these similarities and differences can be accounted for within the two proteins' structure is not yet understood.

Acknowledgments

We thank Dr. James Potter for his gift of troponin C and Dr. Robert Kretsinger (University of Virginia) for sharing his crystallographic data with us and for much helpful discussion. We thank Dr. Melvin Glick (Indiana University School of Medicine) for the use of their Perkin-Elmer atomic absorption spectrometer. Bill Foster at Alltech packed the many different columns for us. The excellent technical assistance of Miguel Carrion is appreciated.

Supplementary Material Available

Two tables listing the HPLC program for the binding assay and a comparison of the primary structure of melittin with three enzyme CaM-binding regions and two figures showing a demonstration of the peak broadening encountered with Tn C at high TFP concentrations and the Hill plot for Tn C (4 pages). Ordering information is given on any current masthead page.

Registry No. TFP, 117-89-5; Ca, 7440-70-2; melittin, 20449-79-0.

References

Anderson, S. R., & Malencik, D. A. (1986) in *Calcium and Cell Function* (Cheung, W. Y., Ed.) Vol. VI, pp 1–42, Academic Press, New York.

Blumenthal, D. K., Takio, K., Edelman, A. M., Charbonneau, H., Titani, K., Walsh, K. A., & Krebs, E. G. (1985) *Proc. Natl. Acad. Sci. U.S.A. 82*, 3187–3191.

Collins, J. H., Potter, J. D., Horn, M. J., Wilshire, G., & Jackman, N. (1973) *FEBS Lett. 36*, 268–272.

Crouch, T. H., & Klee, C. B. (1980) *Biochemistry 19*, 3692–3698.

Dalgarno, D. C., Klevit, R. E., Levine, B. A., Scott, G. M. M., Williams, R. J. P., Gergeley, J., Grabarek, Z., Leavis, P. C., Grand, R. J. A., & Drabikowski, W. (1984) *Biochim. Biophys. Acta 791*, 164–172.

Drabikowski, W., Dalgarno, D. C., Levine, B. A., Gergeley, J., Grabarek, Z., & Leavis, P. C. (1985) *Eur. J. Biochem. 151*, 17–28.

Edelman, A. M., Takio, K., Blumenthal, D. K., Hansen, R. S., Walsh, K. A., Titani, K., & Krebs, E. G. (1985) *J. Biol. Chem. 260*, 11275–11285.

Faust, F. M., Slisz, M., & Jarrett, H. W. (1987) *J. Biol. Chem. 262*, 1938–1941.

Gariépy, J., & Hodges, R. S. (1983) *Biochemistry 22*, 1586–1599.

Giedroc, D. P., Sinha, S. K., Brew, K., & Puett, D. (1985) *J. Biol. Chem. 260*, 13406–13413.

Haiech, J., Klee, C. B., & Demaille, J. (1981) *Biochemistry 20*, 3890–3897.

Harmon, A. H., Jarrett, H. W., & Cormier, M. J. (1984) *Anal. Biochem. 141*, 168–178.

Heidorn, D. B., & Trewhella, J. (1988) *Biochemistry 27*, 909–915.

Herzberg, O., & James, M. N. G. (1985) *Nature 313*, 653–659.

Herzig, J. W., Tkachuk, V. A., Baldenkov, G. N., Feotistov, I. A., Meńshikov, M. Y., & Quast, U. (1987) *Biomed. Biochim. Acta 46*, 5440–5443.

Hidaka, H., Yamaki, T., Naka, M., Tanaka, T., Hayashi, H., & Kobayashi, R. (1980) *Mol. Pharmacol. 17*, 66–72.

Hubbard, S. R., Hodgson, K. O., & Doniach, S. (1988) *J. Biol. Chem. 263*, 4151–4158.

Hummel, J. P., & Dreyer, W. J. (1962) *Biochim. Biophys. Acta 63*, 532–534.

Jackson, A. E., Carraway, K. L., III, Puett, D., & Brew, K. (1986) *J. Biol. Chem. 261*, 12226–12232.

James, P., Maeda, M., Fischer, R., Verma, A. K., Krebs, J., Penniston, J. T., & Carafoli, E. (1988) *J. Biol. Chem. 263*, 2905–2910.

Jarrett, H. W. (1984) *J. Biol. Chem. 259*, 10136–10144.

Jarrett, H. W., Cooksy, K. D., Ellis, B., & Anderson, J. M. (1986) *Anal. Biochem. 153*, 189–198.

Kaetzel, M. A., & Dedman, J. R. (1987) *J. Biol. Chem. 262*, 3726–3729.

Klevit, R. E., Levine, B. A., & Williams, R. J. P. (1981) *FEBS Lett. 123*, 25–29.

Klevit, R. E., Blumenthal, D. K., Wemmer, D. E., & Krebs, E. G. (1985) *Biochemistry 24*, 8152–8157.

Krebs, J., & Carafoli, E. (1982) *Eur. J. Biochem. 124*, 619–627.

Kretsinger, R. H., & Nockolds, C. E. (1973) *J. Biol. Chem. 248*, 3313–3326.

Laemmli, U. K. (1970) *Nature 227*, 680–685.

LaPorte, D. C., Wiermann, B. M., & Storm, D. R. (1980) *Biochemistry 19*, 3814–3819.

Levin, R. M., & Weiss, B. (1978) *Biochim. Biophys. Acta 540*, 197–204.

Lukas, T. J., Burgess, W. H., Prendergast, F. G., Lau, W., & Watterson, D. M. (1986) *Biochemistry 25*, 1458–1464.

Marshak, D. R., Lukas, T. J., & Watterson, D. M. (1985) *Biochemistry 24*, 144–150.

Maulet, Y., & Cox, J. A. (1983) *Biochemistry 22*, 5680–5686.

Newton, D. L., & Klee, C. B. (1984) *FEBS Lett. 165*, 269–272.

Newton, D. L., Burke, T. R., Rice, K. C., & Klee, C. B. (1983) *Biochemistry 22*, 5472–5476.

Newton, D. L., Oldewurtel, M. D., Krinks, M. H., Shiloach, J., & Klee, C. B. (1984) *J. Biol. Chem. 259*, 4419-4426.
Olwin, B. B., & Storm, D. R. (1985) *Biochemistry 24*, 8081-8086.
Perrin, D. D., & Sayce, I. G. (1967) *Talanta 14*, 833-842.
Potter, J. D., & Gergeley, J. (1975) *J. Biol. Chem. 250*, 4628-4633.
Reid, R. E. (1983) *J. Theor. Biol. 105*, 63-76.
Reid, R. E., Gariépy, J., & Hodges, R. S. (1983) *FEBS Lett. 154*, 60-64.
Silver, P. J., Pinto, P. B., & Dachiw, J. (1986) *Biochem. Pharmacol. 35*, 2545-2551.
Steiner, R. F., Marshall, L., & Needleman, D. (1986) *Arch. Biochem. Biophys. 246*, 286-300.
Strynadka, N. C., & James, M. N. (1988) *Proteins 3*, 1-17.
Sundaralingam, M., Bergstrom, R., Strasburg, G., Rao, S. T., Roychodhury, P., Greaser, M., & Wang, B. C. (1985) *Science 227*, 945-948.
Weiss, B., & Levin, R. M. (1978) *Adv. Cyclic Nucleotide Res. 9*, 285-303.
Winkler, M. A., Fried, V. A., Merat, D. L., & Cheung, W. Y. (1987) *J. Biol. Chem. 262*, 15466-15471.
Wyman, J. (1964) *Adv. Protein Chem. 19*, 223-286.

Thermal Denaturation of the Ca^{2+}-ATPase of Sarcoplasmic Reticulum Reveals Two Thermodynamically Independent Domains†

James R. Lepock,* A. Michael Rodahl, Ching Zhang, Miriam L. Heynen, Brenda Waters, and Kwan-Hon Cheng‡
Guelph-Waterloo Program for Graduate Work in Physics, Waterloo Campus, University of Waterloo, Waterloo, Ontario N2L 3G1, Canada

Received July 12, 1989; Revised Manuscript Received August 30, 1989

ABSTRACT: Inactivation of Ca^{2+} uptake and ATPase activity of the Ca^{2+}-ATPase of rabbit sarcoplasmic reticulum was measured and compared to the thermal denaturation of the enzyme as measured by differential scanning calorimetry (DSC) and fluorescence spectroscopy. Two fluorophores were monitored: intrinsic tryptophan (localized in the transmembrane region) and fluorescein isothiocyanate (FITC)-labeled Lys-515 (located in the nucleotide binding domain). Inactivation, defined as loss of activity, and denaturation, defined as conformational unfolding, were irreversible under the conditions used. Activation energies (E_A) and frequency factors (A) for inactivation were obtained for the enzyme in 1 mM EGTA and 1 mM Ca^{2+}. These were transformed to a transition temperature for inactivation, T_m (defined as the temperature of half-inactivation when temperature is scanned upward at 1 °C/min). All denaturation profiles were fit with an irreversible model to obtain E_A and T_m for each transition, and the values of these parameters for denaturation were compared to the values for inactivation. In EGTA, denaturation obeys a single-step model (T_m = 49 °C), but a two-step model is required to fit the DSC provile of the enzyme in 1 mM Ca^{2+}. The specific locations of tryptophan and the fluorescein label were used to demonstrate that denaturation in Ca^{2+} occurs through two distinct thermodynamic domains. Domain I (T_m = 50 °C) consists of the nucleotide binding region and most likely the phosphorylation and transduction regions [MacLennan, D. H., Brandl, C. J., Korczak, B., & Green, N. M. (1985) *Nature 316*, 696-700]. Domain II (T_m = 57-59 °C) consists of the transmembrane region and probably the stalk region. Inactivation of ATPase activity and Ca^{2+} uptake when heated in 1 mM Ca^{2+} is due to denaturation of domain I. Inactivation of ATPase activity (T_m = 49 °C) when heated in 1 mM EGTA is also due to denaturation of domain I, but inactivation of Ca^{2+} uptake (T_m = 37 °C), yielding uncoupling of Ca^{2+} uptake from hydrolysis of ATP, does not correlate with any conformational change in the Ca^{2+}-ATPase detectable by these methods. From these results, it can be inferred that the conformational change occuring during the $E_2 \rightarrow E_1$ transition occurs primarily in domain II (ΔT_m = 8-10 °C), although there is a small stabilization of domain I (ΔT_m = 1 °C), demonstrating interaction and communication between these domains which is necessary for Ca^{2+}-dependent ATPase activity.

The Ca^{2+}-ATPase of sarcoplasmic reticulum (SR) pumps Ca^{2+} using energy derived from the hydrolysis of ATP. These two functions are not inseparable since many treatments uncouple Ca^{2+} transport from ATP hydrolysis, apparently without increasing membrane permeability (Berman, 1982). The ATP binding and phosphorylation sites and the Ca^{2+} binding sites are in diffferent secondary structural domains, as predicted from the primary sequence, but the location of these sites in the tertiary structure is unknown (MacLennan et al., 1985; Brandl et al., 1986; Clarke et al., 1989). Some forms of uncoupling appear to be due to conformational changes in the protein (Berman, 1982), suggesting that the ATPase and Ca^{2+}-translocation activities are located in discrete domains. Ca^{2+} uptake is inactivated rapidly at modest temperatures (near 37 °C) in EGTA while ATPase activity is unaffected at this temperature (McIntosh & Berman, 1978). Addition of Ca^{2+} protects against inactivation of Ca^{2+} uptake. The precise mechanism of inactivation and uncoupling is unknown (Berman, 1982).

The technique of thermal analysis has been profitably applied to the study of many materials, including macromolecules (Donovan, 1984). The general approach is to monitor tran-

†Supported by USPHS Grant CA40251 awarded by the National Cancer Institute, DHHS, to J.R.L. and by grants from the Natural Sciences and Engineering Research Council of Canada.
‡Present address: Department of Physics, Texas Tech University, Lubbock, TX 79409.

0006-2960/90/0429-681$02.50/0